Manuscript submitted to: Volume 1, Issue 1, 31-48.

AIMS Biophysics DOI: 10.3934/biophy.2014.1.31

Received date 10 October 2014, Accepted date 1 December 2014, Published date 4 December 2014

Research article

Metastable capillary filaments in rectangular cross-section open microchannels

Jean Berthier [1,*], Kenneth A. Brakke [2], David Gosselin [1], Maxime Huet [1], Erwin Berthier [3]

1 Department of Biotechnology, CEA/Université Grenoble-Alpes, 17 avenue des Martyrs, 38054, Grenoble, France
2 Mathematics Department, Susquehanna University, 514 University Avenue, Selinsgrove, PA 17870, USA
3 Department of Medical Microbiology and Immunology, University of Wisconsin-Madison, Madison, WI 53705, USA

* **Correspondence:** Email: jean.berthier@cea.fr; Tel: 003-343-878-3551.

Abstract: Spontaneous capillary flow (SCF) in microchannels occurs for specific geometrical and wetting conditions. When the channel walls form corner angles with the channel bottom, liquid filaments may form in the corners. These capillary filaments are often called Concus-Finn (CF) filaments, and they can theoretically spread infinitely.In this work we consider rectangular open U-grooves of varying cross-section width, and we theoretically determine the flow conditions as a function of the aspect ratio of the channel and the liquid-solid contact angle. These flow conditions are numerically checked. Especially, we analyze the configurations where precursor capillary filaments form. We show that these filaments can be metastable, i.e. disappear into a bulk capillary flow if the proper conditions are met. A diagram of the flow regimes is deduced from theoretical developments and checked using numerical modeling.

Keywords: Spontaneous capillary flow (SCF); Concus-Finn filaments (CF); capillary filaments; partial wetting; open-surface microfluidics

1. Introduction

In biotechnology, biology and medicine, point of care (POC) and home care systems are progressively gaining momentum [1–5]. These systems allow for self-testing and telemedicine. Three main types of test are targeted: first, the search for metabolites—such as cholesterol, glucose, thyroid hormones; second, the search for viral load—such as virus and bacteria; third blood

monitoring—such as the measure of INR (prothrombin, thromboplastin and coagulation times) or blood counts. Monitoring at home or at the doctor's office is an important improvement for the patient: the possibility of frequent testing, immediate response, no displacement to the hospital, and monitoring allowed by telemedicine or directly at the doctor's office. Such systems must be low-cost, easily portable, sensitive, and robust.

Let us recall that conventional microfluidic systems use fluids moved by pumps, syringes or electric means, and are not the best solutions when portability and low-cost are an issue. Such systems are bulky and/or require costly, external appliances.

On the other hand, capillary-based systems fulfill the requirements for POC and home-care [2–5]. In these systems, fluids are moved by capillary and surface tension forces. The self-motion of the fluid is called spontaneous capillary flow (SCF). In fact, in such systems the energy source for the fluid motion is the capillary force exerted by the triple line at the front end of the flow. This contrasts with pump or syringe-driven flows, where the motor of the motion is a pump or a syringe usually placed at the back end of the flow.

Capillary systems can be either confined or open, i.e. the fluid moves inside a closed channel [4–6] or in a channel open to the air [7–12]. Although capillary-driven microflows have already been the subject of investigations for space applications [13] and microelectronics [14–16], their main application today is biology and biotechnology. Note that open-surface microfluidic systems are of increasing interest because of their easy and inexpensive fabrication, absence of air bubbles, and their great accessibility.

It has been shown that the aspect ratio (width divided by height) of such channels is an important parameter for the establishment of a spontaneous capillary flow (SCF) [17,18], and it has been shown that capillary precursor filaments may form in sharp corners, depending on the corner angle and on the contact angle [19–21]. These filaments can theoretically extend indefinitely, as long as there is sufficient liquid available, and favorable geometrical conditions [22]. They are frequently called Concus-Finn (CF) filaments, from the name of the first researchers who discovered the phenomenon. Figure 1 shows how CF filaments progressing ahead of the bulk capillary flow may trap undesirable bubbles in confined capillary networks.

CF filaments are also observed in open channels with sharp corners, as shown in Figure 2 for rectangular U-grooves.

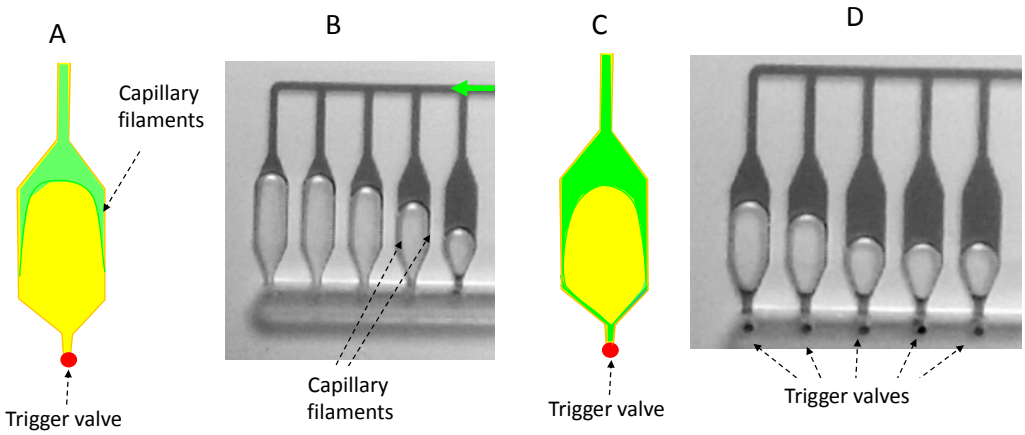

Figure 1. Capillary filaments in a closed (confined) microfluidic network. A: sketch of the advancing liquid (green) in PCR chambers and the capillary precursor filaments; B: start of capillary filling of a hydrophilically-treated PMMA network, with the capillary filaments ahead of the bulk flow; C: sketch of the CF filaments reaching the trigger valve; D: capillary flow stops when the precursor filaments arrive at the trigger valves, and bubbles are imprisoned due to the early arrival of the filaments at the valves (photo courtesy M. Flaender).

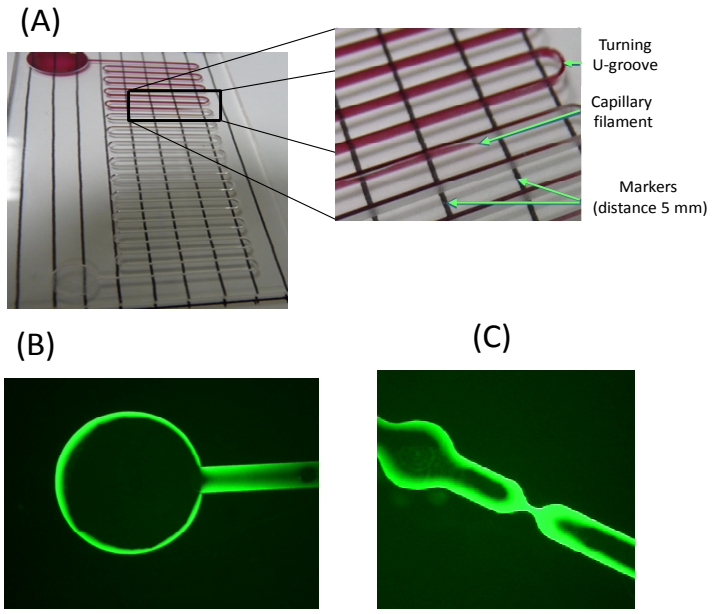

Figure 2. Capillary filaments in open (rectangular) microfluidic channels made of COC (cyclic olefin polymer) hydrophilically treated. A: sketch of the advancing liquid (red) in a long winding U-groove and the capillary precursor filaments at the tip of the flow; B and C: fluorescent precursor capillary filaments in different open geometries.

Let us remark that CF filaments are also of great importance when reagents are present in the liquid: it is observed that there is a spatial correlation between the dry reagent deposition regions and the regions where CF precursor filaments are flowing (figure 3) [9,23].

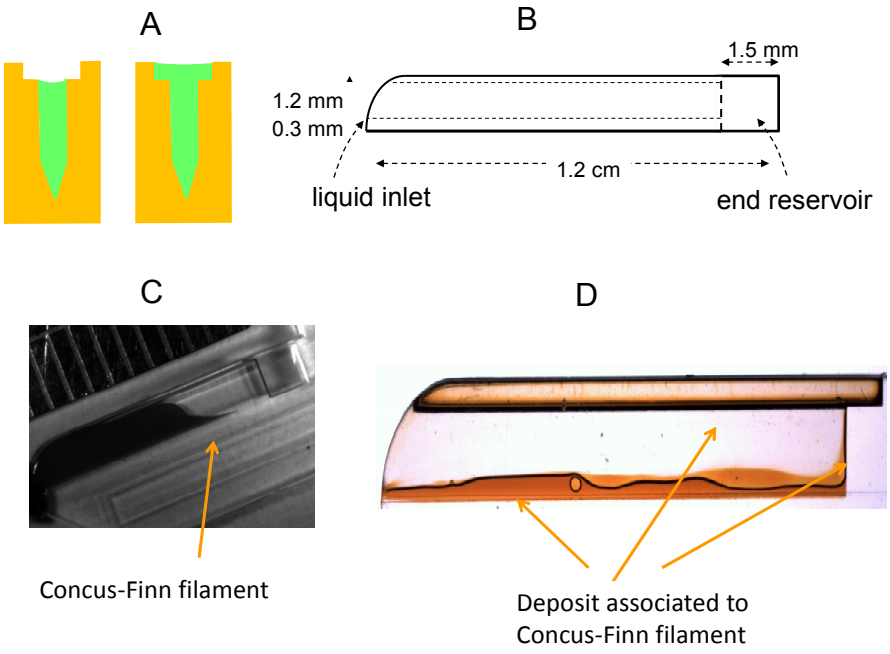

Figure 3. CF filaments in V-shaped channels: (A) cross-section of the device with the capillary filling (in two steps, first the V-slot, then the upper part); (B) side view of the device; (C) capillary flow with CF precursor filament; (D) deposition fluorescein and dextran corresponding to the location of the initial CF locations.

In this work, we restrict our investigations to the different flow regimes that occur in a U-groove of uniform cross-section, depending on the geometrical aspect ratio and the liquid-solid contact angle. A diagram of the flow regimes is theoretically determined and numerically checked with the Surface Evolver numerical program [24]. It is shown that no SCF, bulk SCF (i.e. full channel capillary flow), just capillary filaments in corners, or both SCF and capillary filaments may occur depending on the geometry and contact angle. Moreover, it is shown that the capillary CF filament regime may be metastable. Our approach differs from that of Seemann and colleagues, which only considered droplets in open channels, not SCF [25], but we shall see that there are common features. We finally illustrate the approach by experimental views of the flow regimes.

2. Theoretical approach

We consider here open, rectangular, U-shaped channels of uniform cross-section, and we first present the theoretical approach in the case of a bulk SCF (contact angle above 45°) with no capillary filaments. Then we investigate the case of contact angles smaller than 45°, for which capillary filaments develop.

2.1. SCF in uniform cross-section channels (contact angle > 45°)

Let us first recall the condition that allows for SCF in uniform cross-section channels. Spontaneous capillary flow results when the energy reduction from wetting walls outweighs the energy increase from extending the free surface. In the case of a contact angle larger than 45°—we will give later the justification of this value—the whole width of the bottom plate is wetted or not, depending on a geometrical condition. Using Gibbs' thermodynamic equation [26], it has been shown that the general condition for SCF in composite wall-and-air systems is that the generalized Cassie angle must be less than 90° [17]. Let us recall that the generalized Cassie angle θ^* is the average contact angle defined in the appropriate way, i.e

$$\cos\theta^* = \sum_k \left(f_k \cos\theta_k \right) > 0 , \tag{1}$$

where the θ_k are the Young contact angles with each component k (including air) and the f_k are the areal fractions of each component k in a cross section of the flow (Figure 4). Note that the effective contact angle with air is 180°.

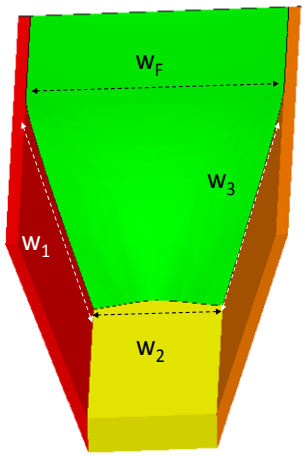

Figure 4. Cross-section of a partly open composite microchannel: the lengths w_i stand for the wetted perimeters and w_F for free perimeter. The areal fractions are $f_i = w_i \Big/ \left(\sum_k w_k + w_F \right)$ **and** $f_F = w_F \Big/ \left(\sum_k w_k + w_F \right)$ **.**

In the case where the walls are composed of a single material (with the same functionalization), relation (1) reduces to

$$\frac{p_F}{p_W} < \cos\theta \quad , \tag{2}$$

where p_F and p_W are respectively the free—in contact with air—and wetted—in contact with wall—

perimeters in a cross section of the channel [21]. Note that the contact angle θ is the static contact angle, with hysteresis if the solid surface is such that there is a contact hysteresis. The dynamic contact angle is not a concern here since the SCF limit occurs at zero—or near zero—velocity.

Using (2), one check that the SCF condition in rectangular cross-section open U-channel is

$$\frac{w}{w+2d} < \cos\theta \ , \tag{3}$$

or

$$q = \frac{w}{d} < \frac{2\cos\theta}{1-\cos\theta} \ . \tag{4}$$

Relation (4) indicates whether the liquid advances in the channel, filling the entire cross section.

2.2. SCF in uniform cross-section channels (contact angle < 45°)

Second, let us recall the condition for filaments to form in dihedrals and corners [19–21]. It has been observed that liquid interfaces in contact with highly wetting solid walls forming a wedge tend to spread in the corner. This behavior results from the fact that the energy decrease from wetting the walls is greater than the energy of the liquid-air interface, so the contact area wants to expand indefinitely, which it can do at low volume by making an ever thinner filament (Figure 5).

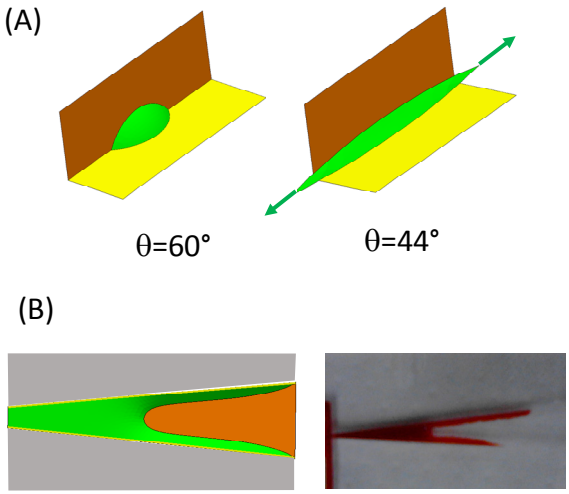

Figure 5. A: a droplet spreads in a 90° corner when the contact angle is less than 45°; B: filaments spread in a diverging, rectangular, open channel. Evolver calculation at the left, experimental view at the right.

Concus and Finn [19] have investigated this phenomenon and they have derived a criterion for capillary motion in the corner of the wedge. If θ is the Young contact angle on both planes and α the

wedge half-angle, the condition for capillary self-motion is

$$\theta < \frac{\pi}{2} - \alpha \,. \tag{5}$$

In the case of a rectangular cross-section, α = 45°, and the contact angle θ should be smaller than 45° to observe filaments.

We now consider the case an open channel with a rectangular cross-section and a contact angle of the liquid with the walls θ < 45°. Two inlet conditions are investigated as shown in Figure 6: first, a large reservoir full of liquid at zero pressure (flat interface); second, a double inlet with separated flows.

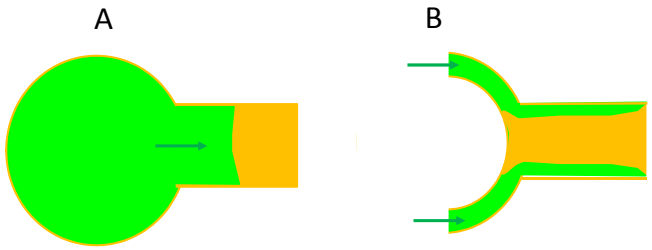

Figure 6. A: liquid inlet from reservoir; B: liquid inlet from separated channels.

2.3. SCF self-dividing into filaments

Let us analyze the case of a straight, rectangular U-groove of large aspect ratio, i.e. $q = w/d >> 1$, where w is the channel width and d is the channel depth. What qualifies as large aspect ratio will be shown to depend on the contact angle, with smaller contact angles leading to higher critical aspect ratios ("critical" meaning the largest aspect ratio compatible with SCF).

This morphology has been experimentally investigated and reported in the literature [27]. In that publication, the rectangular cross-section channel has a height of 8.8 μm and four different widths: 160, 180, 200 and 220 μm (Figure 6). For all these, the aspect ratio is higher than 18. The inlet pressure is supposed to be zero (large reservoir with flat liquid surface).

Analyzing the experimental results, two morphologies of the flow are observed, depending on the value of the aspect ratio (Figure 7). In the first case (1) of the smallest aspect ratio, the channel is completely filled by the fluid, and two filaments advance ahead of the bulk flow. In the second case (2–4), the bulk flow is stopped but two filaments spread in the corners. Figure 8 represent this situation in a cross section.

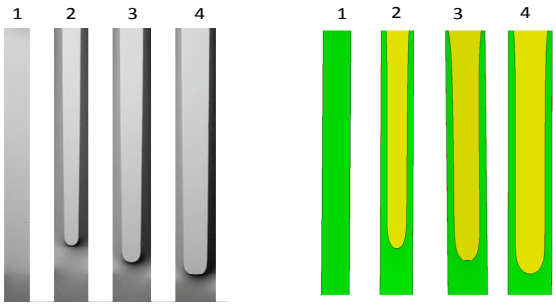

Figure 7. Comparison between experimental results [27] and Surface Evolver numerical results. Channel dimensions: height of walls 8.8 µm, widths of channel: 1–160 µm, 2–180 µm, 3–200 µm, 4–220 µm. The contact angle is 14°.

From a theoretical standpoint, the variation of the surface energy over a distance Δx is different in the two cases: The variation of surface energy in the case of the non-wetted channel center is

$$\begin{aligned}\Delta E_1 = \gamma_{SG}\left(w - 2\frac{d}{\tan\theta}\right)\Delta x \\ + \gamma_{SL}\left(2d + 2\frac{d}{\tan\theta}\right)\Delta x \\ + \gamma_{LG}\left(2\frac{d}{\sin\theta}\right)\Delta x\,,\end{aligned} \tag{6}$$

where γ_{SG}, γ_{SL} and γ_{LG} are respectively the surface tensions between the solid and gas, solid and liquid, and liquid and gas.

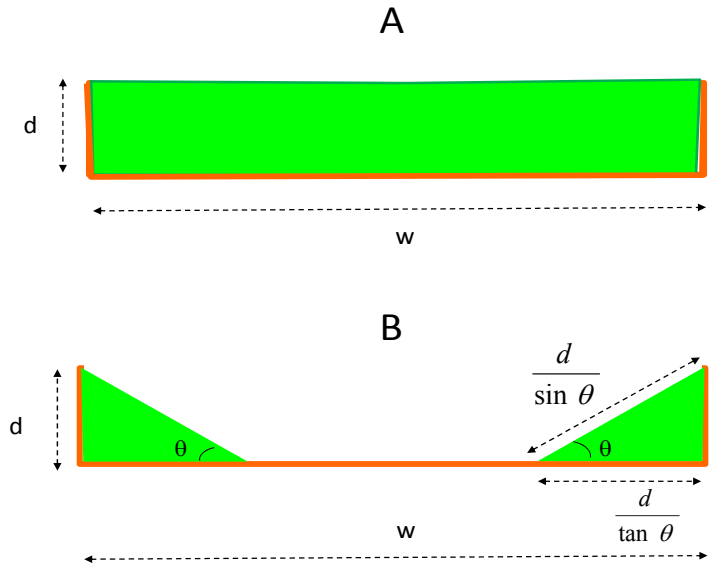

Figure 8. The two morphologies of the capillary flow in a high aspect ratio channel: A, channel completely filled; B, channel partly filled.

In the case of a totally wetted center,

$$\Delta E_2 = \gamma_{SL}(2d + w)\Delta x + \gamma_{LG} w \Delta x \,. \tag{7}$$

The sign of ΔE_1-ΔE_2 indicates whether the center of the channel will be wetted or not. Subtracting (7) from (6) and using the Young relation one finds

$$\Delta E_1 - \Delta E_2 = \gamma_{LG}\,\Delta x\left[\cos\theta\left(w - 2\frac{d}{\tan\theta}\right) + \left(2\frac{d}{\sin\theta} - w\right)\right] . \tag{8}$$

The center of the channel is not wetted if ΔE_1-$\Delta E_2 < 0$, i.e.

$$q = \frac{w}{d} > \frac{2\sin\theta}{1-\cos\theta} \,. \tag{9}$$

If relation (9) is not satisfied, then the smaller surface energy morphology is that of the fully wetted channel. Note that in this case, there are two CF filaments ahead of the bulk flow. Else, if relation (9) is satisfied, the smaller surface energy morphology is that of two separate CF filaments. The bulk flow is stopped just after the outlet of the reservoir but two CF filaments flow separately alongside the walls.

Note that relation (9) involves the contact angle. The capillary filaments are advancing in the channel, and the question is whether a static or dynamic contact angle be considered here, Due to the geometry of the filaments, the advancing front should present a dynamic contact angle, while the side of the filament, in contact with the bottom, is not advancing (nor receding), and a static value of the contact angle is likely. As our concern is the contact area on the bottom plate in a cross section it seems justified using the static contact angle.

Moreover, considering the advancing tip of the filaments, and remarking that the liquid in the middle of the channel is at nearly zero velocity, the filaments advance slowly, due to the effect of the surface tension. Hence their capillary number is very small. Using the empirical correlations of Bracke and colleagues [28], or Seebergh and colleagues [29], based on the capillary number, we find that the difference between the static and dynamic contact angle is less than 1 or 2°. Hence we estimate that the error associated to a constant value of the contact angle is very small.

2.4. Initially separated Concus-Finn filaments

Now consider case B of Figure 8: the fluid inlet is constituted by two separated flows. Two separated Concus-Finn filaments advance in parallel in the open-top channel. In this case, because the pressure is zero, the cross-section of the flow is triangular, and the condition for a filament to continue its motion is given by relation (2).

Using a trigonometric formulation for the free perimeter p_F and the wetted perimeter p_W (Figure 8), relation (2) can be expressed by

$$\frac{p_F}{p_W} = \frac{d}{\sin\theta}\frac{1}{\left(\frac{d}{\tan\theta}+d\right)} = \frac{1}{\sin\theta}\frac{1}{\left(\frac{1}{\tan\theta}+1\right)} = \frac{1}{(\cos\theta+\sin\theta)} < \cos\theta\,. \tag{10}$$

Finally, we obtain

$$\sin\theta < \cos\theta\ , \tag{11}$$

and the condition for motion is $\theta<\pi/4$, which is simply the Concus-Finn condition for perpendicular corners.

On the other hand, using again the triangular shape of the profile in a cross-section, the two filaments stay separated as long as

$$\frac{w}{d} > \frac{2}{\tan\theta}\,. \tag{12}$$

2.5. Metastability of CF filaments

An interesting observation stems from the comparison of relations (9) and (12). It can easily be shown that the inequality

$$\frac{2}{\tan\theta} < \frac{2\sin\theta}{1-\cos\theta} \tag{13}$$

is always true whatever the value of θ. If the value of the aspect ratio q is between the two limits of inequality (13)

$$\frac{2}{\tan\theta} \le q \le \frac{2\sin\theta}{1-\cos\theta}\ , \tag{14}$$

then the channel can sustain either a bulk SCF flow filling the channel or two CF filaments.

The full and filament modes can change in a single channel. This property is illustrated in Figure 9. When the liquid exits the large reservoir, the channel completely fills, and the channel middle is covered with liquid. When the SCF enters a cylindrical enlargement, the flow separates if the cylinder radius is sufficiently large. The condition for observing a dry disc in the middle is derived in the Appendix, based on the catenoidal shape of the liquid surface [21]. The flow is separated into two subflows, and if the cylinder outlet condition satisfies (12), two independent CF filaments continue to flow in the straight outlet channel.

An experimental view of the capillary flow of the liquid in the cylinder is shown in Figure 10, using water marked with a fluorescent dye. The aspect ratio of the channel is w/d=1/4. In this particular case, the outlet channel aspect ratio does not satisfy (12) and the two filaments merge (Figure 11).

In the case of our study (Figure 9), relation (14) is satisfied because downstream of the cylinder the geometrical dimensions are the same as upstream of the cylinder. The analysis of section 2.4 stands and two separate CF filaments flow in the channel. The two filaments are independent, they never merge and the middle of the channel is never wetted.

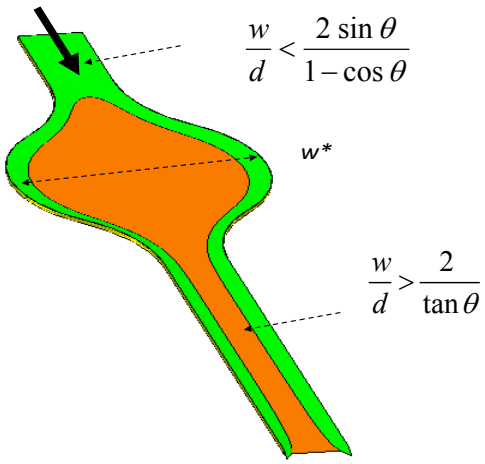

Figure 9. Capillary flow in a shallow open channel: at the top, the liquid enters the whole channel and the channel is progressively completely filled with liquid. The large cylindrical part acts as a separator for the flow, and two filaments continue in the channel past the cylinder.

However, this morphology is metastable: if the two filaments are forced to contact each other, the fully wetted situation is restored, as shown in Figure 12. Note that the restoration of the fully wetted morphology also progresses backward towards the large cylinder.

The corresponding experimental result is shown in figure 13: A neck in the channel forces the separated subflows to merge. The merged part then extends in the two directions, upstream and downstream.

3. Results and Discussion

We have seen in section 2.1 that the SCF conditions in rectangular cross-section open U-channel, when the contact angle is larger than 45°, is $q = w/d < 2\cos\theta/(1-\cos\theta)$. In such a case, there is no formation of capillary filaments because the CF limit (5) is not respected.

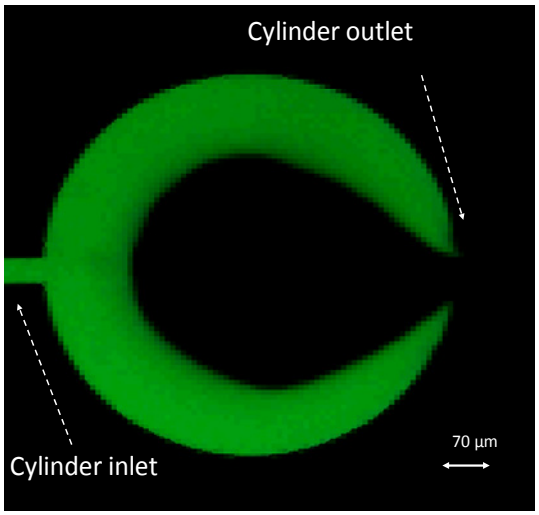

Figure 10. Experimental view of fluorescent water flow in a wide cylinder; the flow separates in two filaments advancing alongside the curved corners. The substrate is etched in silicon and coated with a SiO_2 layer (contact angle 43°). The height of the walls is 200 µm, and the diameter of the cylinder is 1000 µm. The channel width is 50 µm.

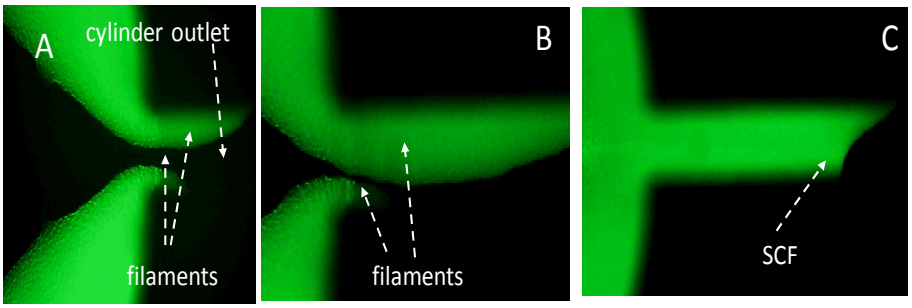

Figure 11. View of fluorescent water flowing out of a wide cylindrical cavity. A: the two CF filaments enter the cylinder outlet; B: the filaments grow laterally to reach their nominal width; C: because relation (10) is not satisfied, the two filaments merge and a bulk SCF is observed.

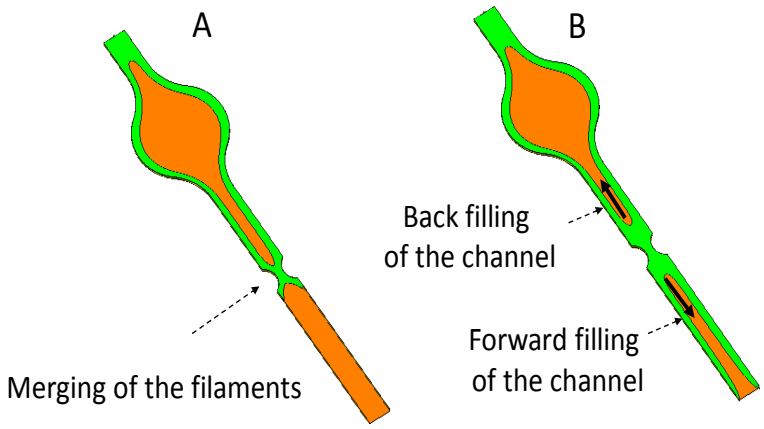

Figure 12. Same as Figure 8, but the two filaments are forced to contact downstream from the cylinder, and a fully wetted morphology is restored.

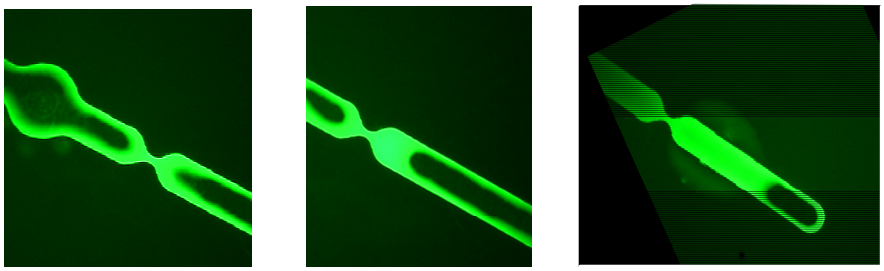

Figure 13. Capillary filaments of fluorescent water forced to merge in a neck in the channel. The substrate is made of PMMA, hydrophilically treated by exposition to plasma O_2. The contact angle is approximately 30°; the height of the walls is 100 µm, and the width of the channel is 500 µm; the aspect ratio is 5 and satisfies (12).

For an aspect ratio not respecting (14), neither bulk SCF nor capillary filaments are observed.

When the contact angle is smaller than 45°, the situation is more complicated: (1) above the limit $q > 2\sin\theta/(1-\cos\theta)$, no bulk SCF is observed, but two CF filaments spread in the corners; (2) below the limit $q < 2/\tan\theta$ bulk SCF is observed preceded by CF filaments; (3) for an aspect ratio between $2/\tan\theta \le q \le 2\sin\theta/(1-\cos\theta)$, the situation is metastable and depends on the history of the flow: either separated CF filaments progress in the channel, or a full SCF occurs preceded by two CF filaments.

All the above conditions are shown in Figure 14. It is interesting to compare Figure 13 with the experimental and numerical results obtained by Seemann and colleagues for a liquid drop placed in a rectangular open U-groove [25]. In their representation, the axes (aspect ratio vs. contact angle) are inverted and the aspect ratio is also inverted. But the two theoretical curves (green and red) of Figure

13 corresponding to the relations $q = 2\sin\theta/(1-\cos\theta)$ for $\theta < 45°$ and $q = 2\cos\theta/(1-\cos\theta)$ for $\theta > 45°$ are identical to the experimental curves of [25].

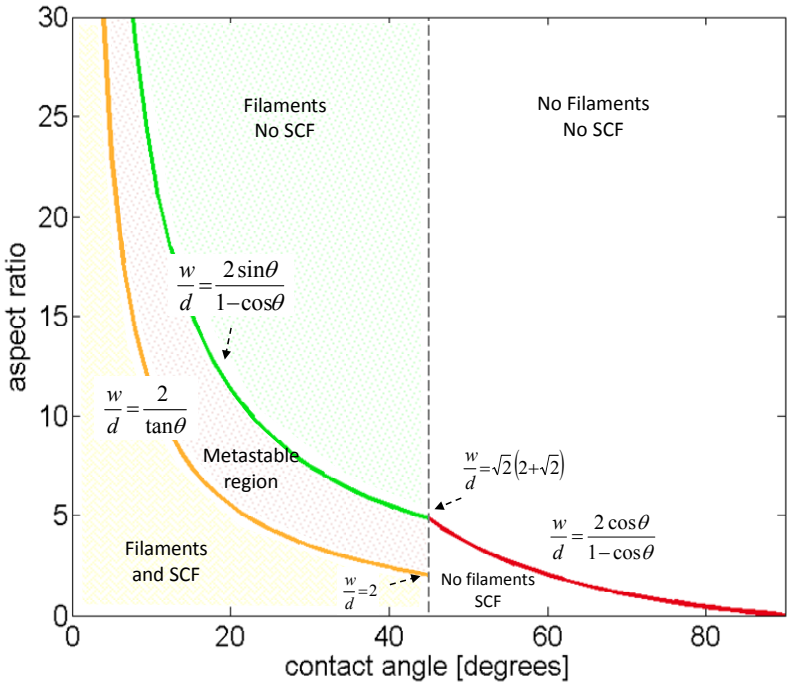

Figure 14. The different capillary flow domains for a rectangular, open-surface capillary channel: the notation "SCF" means that the bulk is advancing in the channel, and the notation "filaments" means that two CF filaments progress alongside the interior corners.

4. Conclusion

Capillary filaments—or Concus-Finn filaments—often appear in microsystems treated hydrophilically. These filaments can have a very large extension, as long as there is liquid available and the geometry of the corners continues. Sometimes they are a drawback because of an unwanted loss of liquid, or an undesirable propagation of liquid. Sometimes they are useful, because they boost the velocity of the capillary flow [9]. Moreover, they can flow alone while the bulk of the liquid is at rest, or precede the bulk of the liquid.

In this work, the appearance of such filaments and their stability has been studied for a rectangular cross-section, open channel. The conditions under which they appear have been determined, together with their stability and their association to the capillary motion of the bulk flow.

Appendix: capillary flow in a cylindrical cavity

When a SCF arrives in a cylindrical cavity, three flow configurations are possible: (1) the SCF stops, (2) the SCF entirely fills the cavity, (3) filaments fill the bottom corners and the liquid surface

has approximately the shape of a catenoid, with the center of the cylinder staying dry [20]. These configurations depend on the radius of the cylinder and the contact angle. In the case of a contact angle under 45°, only the two last cases are possible. Let us analyze the condition for observing a catenoid (Figure 15).

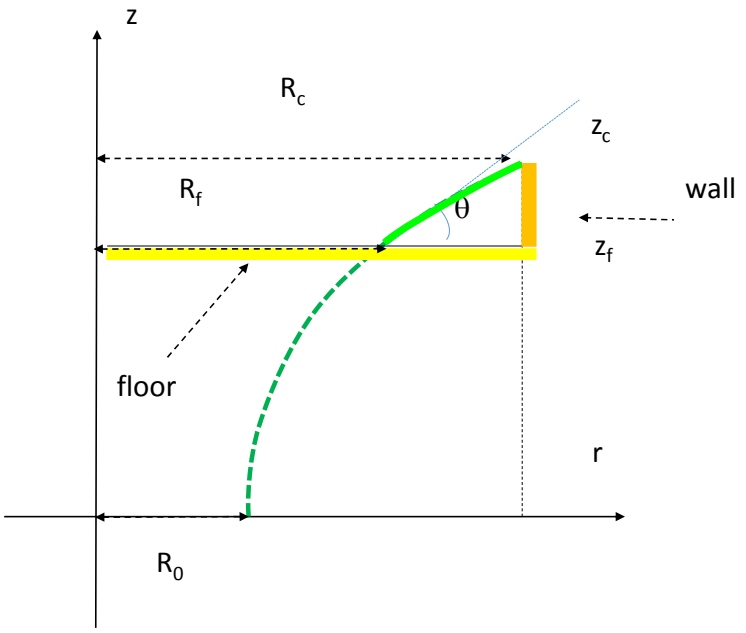

Figure 15. Sketch of the catenoid cross-section representing the surface of the fluid (continuous green line) and the cylinder walls (orange) and floor (yellow). The contact angle between the liquid and the floor is θ. Remark that z_c-z_f = h is the height of the wall.

A catenoid is a zero-pressure surface shape with cylindrical symmetry. The liquid surface shape in the cylindrical enlargement of a channel is not exactly a catenoid, due to the entry and exit openings, but because the liquid in the openings is below the wall height, a catenoid with the height of the wall and the same contact angle on the floor will act as a barrier beyond which the liquid will not pass.

The equation of a catenoid with a neck defined by $z = 0$, $R = R_0$, is

$$r = R_0 \cosh\left(\frac{z}{R_0}\right). \tag{15}$$

The first condition to determine R_0 is the slope at the contact with the floor: at the floor level ($z = z_f$) the tangent to the catenoid has a slope dz/dr = tanθ, so

$$\frac{dr}{dz} = \sinh\left(\frac{z_f}{R_0}\right) = \frac{1}{\tan\theta}, \tag{16}$$

hence

$$\frac{z_f}{R_0} = \operatorname{arcsinh}\left(\frac{1}{\tan\theta}\right). \tag{17}$$

The second condition is the contact at the top, on the edge of the cylinder,

$$R_c = R_0 \cosh\left(\frac{z_c}{R_0}\right) = R_0 \cosh\left(\frac{z_f}{R_0} + \frac{h}{R_0}\right) \quad . \tag{18}$$

Substitution of (17) in (18) yields

$$R_c = R_0 \cosh\left(\operatorname{arcsinh}\left(\cot\theta\right) + \frac{h}{R_0}\right) \quad , \tag{19}$$

which is an implicit solution for R_0. There is a critical value for R_c below which there are no solutions to (19), and above which there are two solutions for R_0, the larger of which is the stable catenoid of interest. We denote that stable solution $R_0 = f(\theta, h)$. The floor level is given by (17) using the value of R_0

$$\frac{z_f}{R_0} = \frac{z_f}{f(\theta,h)} = \operatorname{arcsinh}\left(\frac{1}{\tan\theta}\right) \quad , \tag{20}$$

and using the relation $\cosh^2(z) - \sinh^2(z) = 1$, the radius of the dry disc in the middle of the cylindrical cavity is then

$$R_f = \left(1 + \cot^2\theta\right) f(\theta,h). \tag{21}$$

Hence, if R_c is greater than the critical value and the liquid enters the cylinder through its ingress opening, a dry disc remains in the middle of the cylinder. This is the case of Figure 9. If the outlet of the cylinder is wider than condition (10), the liquid remains separated in two parts on egress, and two CF filaments continue to advance in the outlet channel.

Acknowledgements

We thank Melanie Flaender, Noémie Villard, Catherine Pudda, and François Boizot from the CEA-Leti, for their help achieving the microflabrication of the capillary devices. We also acknowledge the Biotechnology Department of the CEA-Leti for the funding of this work.

References

1. Kost GJ (2002) Principles and Practice of Point-of-Care Testing. Hagerstwon, MD: *Lippincott Williams & Wilkins* 3–12.
2. Yager P, Edwards T, Fu E, et al. (2006) Weigl, Microfluidic diagnostic technologies for global public health. Nature 442(7101): 412–418.
3. Martinez AW, Phillips ST, Whitesides GM (2010) Diagnostics for the developing world: microfluidic paper-based analytical devices. Anal Chem 82: 3–10.
4. Gervais L, de Rooij N, Delamarche E (2011) "Microfluidic chips for point-of-care immunodiagnostics". Adv Mater 23 (24): H151–H176.
5. Gervais L, Delamarche E (2009) Toward one-step point-of-care immunodiagnostics using capillary-driven microfluidics and PDMS substrates. Lab Chip 9: 3330–3337.
6. Safavieh R, Juncker D (2013) Capillarics: pre-programmed, self-powered microfluidic circuits built from capillary elements. Lab Chip 13: 4180–4189.
7. Satoh W, Hosono H, Suzuki H (2005) On-Chip Microfluidic Transport and Mixing Using Electrowetting and Incorporation of Sensing Functions. Anal Chem 77: 6857–6863.
8. Casavant BP, Berthier E, Theberge AB, et al. (2013) Suspended microfluidics. Proc Natl Acad Sci 110 (25): 10111–10116.
9. Berthier J, Brakke KA, Furlani EP, et al. (2014) Whole blood spontaneous capillary flow in narrow V-groove microchannels. Sensor Actuat B-Chem [impress].
10. Berthier J, Brakke KA, Gosselin D, et al. (2014) Suspended microflows between vertical parallel walls. Microfluid Nanofluid [impress].
11. Tung CK, Krupa O, Apaydin E, et al. (2013) A contact line pinning based microfluidic platform for modelling physiological flows. Lab Chip 13: 3876–3885.
12. Cox RG (1983) The spreading of a liquid on a rough solid surface. J Fluid Mech 131: 1–26.
13. Chen YK, Melvin LS, Rodriguez S, et al. (2009) Weislogel, Capillary driven flow in micro scale surface structures. Microelectron Eng 86: 1317–1320.
14. Rye RR, Yost FG, Mann J (1996) Wetting Kinetics in Surface Capillary Grooves. Langmuir 12: 4625–4627.
15. Romero LA, Yost FG (1996) Flow in an open channel capillary. J Fluid Mechanics 322: 109–129.
16. Yost FG, Rye RR, Mann JA (1997) Solder wetting kinetics in narrow V-grooves. Acta Materialia 45: 5337–5345.
17. Berthier J, Brakke KA, Berthier E (2014) A general condition for spontaneous capillary flow in uniform cross-section microchannels. Microfluid Nanofluid 16: 779–785.
18. Ouali FF, McHale G, Javed H, et al. (2013) Wetting considerations in capillary rise and imbibition in closed square tubes and open rectangular cross-section channels. Microfluid Nanofluid 15: 309–326.
19. Concus P, Finn R (1969) On the behavior of a capillary surface in a wedge. Proc Natl Acad Sci 63(2): 292–299.
20. Concus P, Finn R (1994) Capillary surfaces in a wedge—differing contact angles. Microgravity Sci Tec 7: 152–155.
21. Berthier J, Brakke KA (2012) The physics of microdrops. Scrivener-Wiley publishing.
22. Brakke KA (1992) Minimal surfaces, corners, and wires. J Geom Anal 2: 11–36.
23. Girardo S, Cingolani R, Chibbaro S, et al. (2009) Corner liquid imbibition during capillary penetration in lithographically made microchannels. Appl Phys Lett 94: 171901–171901–3.
24. Brakke KA (1992) The Surface Evolver. Exp Math 1(2): 141–165.

25. Seemann R, Brinkmann M, Kramer EJ, et al. (2005) Wetting morphologies at microstructured surfaces. Proc Natl Acad Sci 102(6): 1848–1852.
26. Gibbs JW (1873) A method of geometrical representation of the thermodynamic properties of substances by means of surfaces. T Connecticut Academy Arts Sciences 2: 382–404.
27. Jokinen V, Franssila S (2008) Capillarity in microfluidic channels with hydrophilic and hydrophobic walls. Microfluid Nanofluid 5: 443–448.
28. Bracke M, De Voeght E, Joos P (1989) The kinetics of wetting: the dynamic contact angle. Progr Colloid Polym Sci 79:142–149.
29. Seebergh JE, Berg JC (1992) Dynamic wetting in the low capillary number regime. Chem Eng Sci 47 (17): 4455–4464.